Cluster decimation derivation of exact percolation-thermal crossover exponent in dilute spin models

1983 J. Phys. A: Math. Gen. 16 1289

(http://iopscience.iop.org/0305-4470/16/6/023)

J. Phys. A: Math. Gen. **16** (1983) 1289–1306. Printed in Great Britain

Cluster decimation derivation of exact percolation–thermal crossover exponent in dilute spin models

R B Stinchcombe

Department of Theoretical Physics, 1 Keble Road, Oxford OX1 3NP, UK

Received 6 September 1982, in final form 11 October 1982

Abstract. It is shown that the decimation method of renormalisation group theory in a restricted parameter space, applied to *any* cluster, gives the exact unit value for the percolation–thermal crossover exponent for bond-diluted Ising, Potts and anisotropic Heisenberg models.

1. Introduction

The percolation–thermal crossover exponent ϕ plays a key role in the behaviour of dilute spin systems. As described at the beginning of § 2 it determines the shape of the phase boundary at the percolation threshold, at which the transition temperature falls to zero, and it governs the competition between the geometric and thermal factors limiting the divergence of the correlation length and, through it, the critical properties near the threshold.

Renormalisation group theory gives a framework in which such exponents can be obtained. Normally approximate values are obtained, usually by stopping at some finite order in the epsilon or loop expansion, or by working with the real-space renormalisation methods on simple clusters. In the case of the percolation–thermal crossover exponent, however, the earliest cluster calculation for a dilute spin model (Young and Stinchcombe 1976) gave unit result for ϕ, as did subsequent calculations on different specific clusters (Jayaprakash *et al* 1978, Yeomans and Stinchcombe 1978, 1979, Stinchcombe 1982 and references therein). Using the ε expansion, Stephen and Grest (1977) and Wallace and Young (1978) succeeded in proving that the unit value for the crossover exponent remains for dilute Ising and Potts models to all orders in the ε expansion:

$$\phi = 1. \tag{1}$$

The purpose of the present paper is to show that the result (1) is also obtained by a proper application of the real-space (cluster decimation) method, independently of the nature and size of the cluster used, with the use of a restricted parameter space. The result is true for bond-diluted systems of Ising, Potts and anisotropic Heisenberg types.

The physical reason for the result is closely related to that underlying the derivation of ϕ given by Coniglio (1981a, b), which considers the nature of the backbone of the incipient infinite cluster at the percolation threshold, and directly evaluates the average susceptibility on the incipient infinite cluster. Though Coniglio's discussion is based

on cluster statistics while ours concerns the real-space renormalisation group scheme, both depend on the limiting role played at low temperatures near the percolation threshold by the effect of one-dimensional paths. Our discussion also explains why the real-space renormalisation group (RSRG) method, even on simple clusters, can be so effective in dealing with dilute systems.

The structure of the paper is as follows. In § 2 we briefly introduce the basic ideas and notation of percolation–thermal crossover in dilute spin systems, and its treatment by renormalisation group procedures. In § 3 we give some preliminary general development and illustrate with simple examples based on specific clusters the main steps behind the RSRG procedure. This serves as an introduction to the general treatment given in § 4, which shows that independently of the cluster used and of another customary approximation (the 'first moment' approximation) the RSRG method for bond-diluted Ising models will always lead to unit value for ϕ. Section 5 is a brief discussion including an extension of the treatment to bond-diluted Potts and anisotropic Heisenberg systems.

2. Crossover near the percolation threshold in dilute systems

The phase boundary separating ordered from paramagnetic regimes in a simple dilute magnet is shown schematically in figure 1. Throughout this paper we shall be concerned with the neighbourhood of the percolation threshold A, where the concentration p takes the critical value p_c, and temperature T is zero. It is simplest for us to consider here only (quenched) bond dilution, where p is the concentration of non-zero exchange bonds: site dilution has, by universality, the same critical exponents.

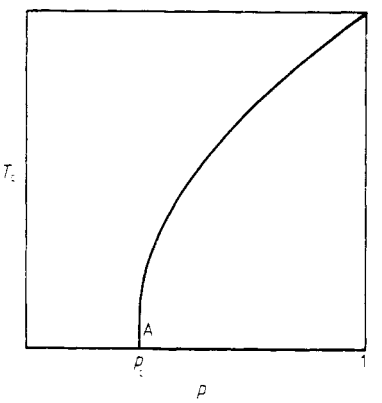

Figure 1. Schematic phase diagram of temperature against concentration for a diluted magnet, showing the percolation fixed point A.

As A is approached from any direction the correlation length ξ diverges, and this divergence induces the critical behaviour of the system. The purely geometric (percolation) divergence at zero temperature is the divergence of connectivity length scale associated with the appearance of the infinite cluster of connected spins:

$$\xi \propto |p - p_c|^{-\nu_p} \qquad p \sim p_c, \quad T = 0. \tag{2}$$

The divergence of ξ as the temperature is reduced to zero at $p = p_c$ is a thermal effect related to the spin correlations on the incipient infinite cluster:

$$\xi \propto \varepsilon^{-\nu_t} \qquad T \sim 0, \quad p = p_c. \tag{3}$$

In (3) we have introduced the appropriate characteristic low-temperature variable for the spin system, which is

$$\varepsilon(T) = 2\exp(-2J/k_B T) \tag{4}$$

in the case of spin-$\frac{1}{2}$ Ising systems, and has a closely related (exponential) form, to be given in § 5, for Potts models and anisotropic Heisenberg systems.

Equations (2) and (3) are special cases of the general critical dependence of ξ on concentration and temperature, which is expressed through a scaling form in terms of the two scaling fields $|p - p_c|^{\nu_p}$ and ε^{ν_t}:

$$\frac{1}{\xi} = \varepsilon^{\nu_t} \Phi\left(\frac{|p - p_c|^{\nu_p}}{\varepsilon^{\nu_t}}\right). \tag{5}$$

In place of the function Φ, a related scaling function with argument $|p - p_c|^{\phi}/\varepsilon$ can be used. ϕ is the crossover exponent given by

$$\phi = \nu_p / \nu_t. \tag{6}$$

Any pair of the three exponents ν_t, ν_p and ϕ gives the critical dependence of ξ, and through it the whole thermal–geometrical critical behaviour of the system. Of particular importance is the crossover exponent ϕ since this governs the competition between the thermal and geometrical influences on the critical behaviour, and in particular determines the shape of the critical curve near the percolation threshold. The critical curve, along which ξ diverges, is (from (5)) where the argument of Φ takes the particular value corresponding to a zero of Φ, so the critical temperature T_c is given by

$$\varepsilon(T_c) \propto |p - p_c|^{\phi}. \tag{7}$$

Two parameters, p and T, are required for the description of the diluted system, if we ignore field dependence, anisotropy and other generalisations. The renormalisation group procedure is to consider the transformation of such parameters under a change of length scale of the system (dilatation by scale factor b, say). In the Ising case, where the most convenient thermal variable is, instead of T,

$$t = \tanh J/k_B T \tag{8}$$

(with J the exchange constant), the parameter transformation under dilatation by b takes the form $p \to p'$, $t \to t'$, where

$$p' = R(p) \tag{9}$$

$$t' = Q(p, t). \tag{10}$$

We have taken here a simple situation, such as those considered in the next section, where the dilatation involves no increase of parameter space, i.e. the generation of new couplings and correlation has been ignored. The fact that the right-hand side of (9) does not involve the thermal variable t is because in such quenched dilution problems the probability p' of nearest neighbour connections on the scaled lattice is determined geometrically.

Standard arguments (Wilson and Kogut 1974, Stinchcombe 1982) then give the percolation threshold A ($p = p_c$, $t = 1$) as a fixed point of the transformations (9) and (10), and the exponents ν_p and ν_t are given as follows in terms of the eigenvalues λ_p and λ_t of the transformations (9) and (10) linearised in the neighbourhood of this fixed point:

$$b^{1/\nu_p} = \lambda_p \tag{11}$$

$$b^{1/\nu_t} = \lambda_t \tag{12}$$

where

$$\lambda_p = \left.\frac{dR(p)}{dp}\right|_{p=p_c} \tag{13}$$

$$\lambda_t = \left.\frac{\partial Q}{\partial t}\right|_{p=p_c, t=1}. \tag{14}$$

It can be seen from (11) and (12) that if

$$\lambda_p = \lambda_t \tag{15}$$

it follows that the crossover exponent ϕ (equation (6)) is unity, as expressed by (1). The aim of this paper is to derive (15), and hence (1), by application of RSRG procedures on any cluster.

The next section (§ 3) gives some general preliminary discussion, and shows how (15) follows in the usual RSRG treatments of bond-diluted systems using specific clusters; § 4 shows that the result is quite general, not dependent on the clusters used, nor on the usual 'first moment' approximation also used in § 3.

3. General preliminaries and illustrations of how $\phi = 1$ follows from RSRG on specific clusters

Two approximations are normally used in RSRG treatments of dilute spin systems.

(i) Restriction of the calculation to a specific simple cluster.

(ii) Scaling of the distribution of random exchange interactions back to the original binary form by using a first moment approximation on the thermal variable t. (This is explained in detail in § 4.)

Young and Stinchcombe (1976) showed, using specific clusters (approximation (i)), that equal results are obtained for the percolation and thermal eigenvalues λ_p and λ_t, leading to unit value for ϕ. Other derivations of this result, using approximations (i) and (ii), have been given by subsequent authors (Jayaprakash *et al* 1978, Yeomans and Stinchcombe 1978, 1979). In this section we illustrate this point with selected examples. The examples are chosen to introduce the basic ideas and notation needed for the removal of restriction (i), which is the most difficult point to be covered by the general discussion of § 4. Section 4 also removes restriction (ii); the original paper by Young and Stinchcombe (1976) also shows in a different way that it is an inessential restriction.

The usual RSRG method for dilute spin systems, introduced by the above authors and reviewed by Stinchcombe (1982), is to arrive at the transformations (9) and (10) by decimation of spins employing the two approximations (i) and (ii) above.

The simplest non-trivial cluster to use is that shown in figure 2 for the square lattice. Then the total probability of linkage from A to B (via 1 and/or 2) is

$$p' = 2p^2 - p^4 \equiv R(p), \tag{16}$$

while the effective strength t' of the renormalised bond connecting A and B is given by

$$p't' = 2p^2(1-p^2)t^2 + p^4\frac{2t^2}{1+t^4} \equiv p'Q(p,t). \tag{17}$$

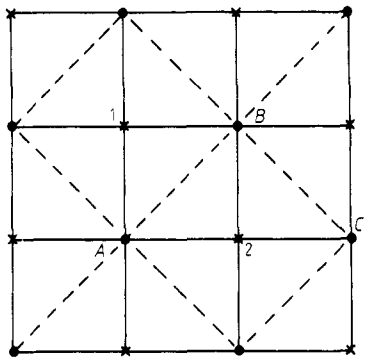

Figure 2. Dilatation of the square lattice: undecimated spins $A, B, C, \ldots$ lie on a new square lattice shown by broken lines, larger by a scale factor $b = \sqrt{2}$. $A1B2$ is the simplest cluster, containing a single 'renormalised' bond, joining spins A and B of the new lattice.

The percolation threshold for this simple description is given as the fixed point of (16) ($p_c = 0.618\ldots$) and the transformations (16) and (17) linearised in the neighbourhood of the fixed point $p = p_c$, $t = 1$ have eigenvalues

$$\lambda_p = \lambda_t = 4p_c(1-p_c^2). \tag{18}$$

So this simple example gives $\phi = 1$ (Young and Stinchcombe 1976).

In writing down (16) and (17) we used both a specific simple cluster (figure 2) and the first moment approximation which was needed to obtain (17). It may seem that the result $\lambda_p = \lambda_t$ is a coincidence for this special cluster, since the above discussion fails to bring out any basic reason for the result. To see that there is an underlying structure responsible for the result, and its generalisation to arbitrary clusters, we now introduce some general formalism and preliminaries, and then give a few more specific examples to indicate the patterns which give the hints for a general result.

We need to adopt some scheme for distinguishing cluster configurations, that is, for a given configuration which bonds of the cluster are present and which are absent. It will turn out that three different but related schemes will be useful. The simplest (scheme 1) is to distinguish configurations by drawing as, say, wavy lines those bonds which are present and leaving blank any bond which is absent. Different diagrams then correspond to independent probabilistic 'events' and their probabilities can be summed. In a second scheme (scheme 2) all series paths joining the undecimated spins A and B are drawn, together with all their possible intersections, and their probabilities are combined by the inclusion–exclusion principle (Feller 1968). In this

case, full lines denote bonds which are present (probability p) and blanks denote bonds whose occupation is not specified. A third scheme will be introduced later.

For some such labelling we suppose that the bond configurations of the cluster are labelled by $\alpha = 1, 2, \ldots$ and the associated probabilities are denoted by $P_\alpha(p)$. In scheme 1, $P_\alpha(p)$ is $p^{N_\alpha}(1-p)^{M_\alpha}$ where N_α and M_α are the numbers of wavy and blank lines in the diagram representing configuration α, while in scheme 2 the probability $P_\alpha(p)$ will be p^{n_α} with n_α the number of full lines in the representation of configuration α. We shall also need for each configuration α the quantities S_α and $T_\alpha(t)$, where S_α is 1 if the configuration gives a linkage (a path of present bonds) from A to B and zero otherwise, and where $T_\alpha(t)$ is the contribution from configuration α to the tanh variable representing the exchange coupling between the spins at sites A and B.

Then, summing over all configurations on the cluster being used,

$$p' = R(p) = \sum_\alpha P_\alpha(p) S_\alpha \tag{19}$$

$$p't' = p'Q(p,t) = \sum_\alpha P_\alpha(p) T_\alpha(t). \tag{20}$$

The last equation employs approximation (ii), since it gives the weighted average of the contributions of the different configurations to the tanh variable representing the exchange coupling.

Scheme 1 is presented in this paper because it is the easiest to understand and because it leads to a relationship for the evaluation of $T_\alpha(t)$. Scheme 2 is used because it is the easiest scheme in which to evaluate the (percolation) eigenvalue of the transformation (19). The third scheme, which is much less obvious than the other two, will be needed to provide an alternative to scheme 1, in which $T_\alpha(t)$ can still be simply evaluated yet contact can be made with scheme 2 so that the equivalence of λ_p and λ_t can be shown in general (§ 4).

From the concentration transformation in the form (19), the fixed point p_c is given by

$$p_c = \sum_\alpha P_\alpha(p_c) S_\alpha \tag{21}$$

and the percolation eigenvalue by

$$\lambda_p = \sum_\alpha P'_\alpha(p_c) S_\alpha. \tag{22}$$

In the thermal scaling (20) we first consider the zero-temperature situation ($t = 1$). Any configuration α giving a connecting path provides a non-zero exchange between A and B and at zero temperature this makes the resulting contribution T_α to the tanh variable equal to unity; if configuration α provides no connection the exchange and related tanh variable contributions are zero. So from this zero-temperature consideration

$$T_\alpha(1) = S_\alpha. \tag{23}$$

Thus inserting $t = 1$ into the right-hand side of (20) gives

$$p't' = \sum_\alpha P_\alpha(p) S_\alpha = p', \tag{24}$$

making t' also unity. Therefore $t = 1$ is a fixed point of (20), as required to give the zero-temperature percolation fixed point A of figure 1. This is the fixed point of

interest in the crossover considerations of this paper, and the linearisation about this fixed point is needed to obtain the thermal eigenvalue. For this, we introduce the notation

$$t = 1 - \varepsilon \qquad \varepsilon \ll 1. \tag{25}$$

ε is then as defined in (4). Then, writing the Taylor series $T_\alpha(1-\varepsilon)$ to first order and using (23) for the zeroth-order term,

$$T_\alpha(1-\varepsilon) = S_\alpha - \varepsilon T'_\alpha(1) + \ldots. \tag{26}$$

Inserted into (20) this gives, using (14),

$$\lambda_t = \frac{1}{p_c} \sum_\alpha P_\alpha(p_c) T'_\alpha(1). \tag{27}$$

We now discuss the use of schemes 1 and 2 in the evaluation of the eigenvalues (22) and (27). This, and the nature of the two schemes, is best illustrated by an example, and for this we take the cluster of figure 2. The different configurations of this cluster are represented in scheme 1 by the diagrams of figure 3. The first nine diagrams do not provide a linkage from A to B and so do not contribute to (19) and (20). So we may consider only those diagrams, labelled $\alpha = 1, 2, \ldots 7$, which do provide a linkage ($S_\alpha = 1$). Diagrams of the three topologically distinct types $\alpha = 1$, 2, $\alpha = 3$, 4, 5, 6, and $\alpha = 7$ have individual probabilities $p^2(1-p)^2$, $p^3(1-p)$ and p^4, so adding the probabilities of the seven independent events to obtain (19) we recover the result (16) and hence the percolation eigenvalue given in (18). The direct evaluation of (22) in scheme 1 turns out not to be convenient for us (see below). The direct evaluation of (27) is, however, very convenient in this scheme: this is because it is possible to show (appendix 1) that if the diagram α links A and B then

$$T'_\alpha(1) = r_\alpha \tag{28}$$

where r_α is the number of single bonds in the diagram α whose removal would disconnect A and B. This is essentially because a series path of r bonds gives a contribution t^r to the tanh of the effective exchange, while any parallel constituent in a path increases the effective exchange for that part of the path and this more strongly coupled part is less affected by the variation ε of t in (26). For the diagrams of figure 3,

$$r_1 = r_2 = r_3 = r_4 = r_5 = r_6 = 2 \qquad r_7 = 0. \tag{29}$$

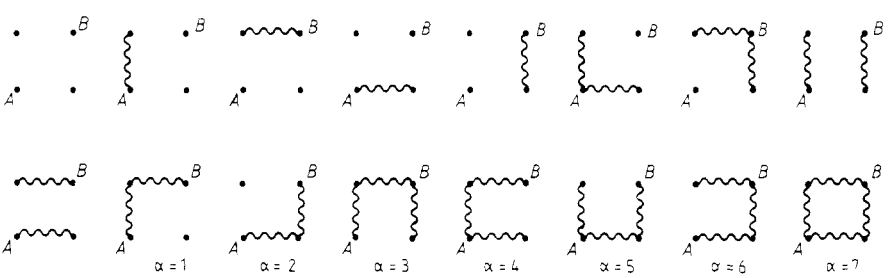

Figure 3. Diagrams of scheme 1 representing the configuration of the simple cluster of figure 2.

So for the cluster of figure 2 the evaluation of (27) takes the form

$$\lambda_t = \frac{1}{p_c} \sum_{\alpha} P_\alpha(p_c) r_\alpha S_\alpha \tag{30}$$

$$= \frac{1}{p_c} [p_c^2(1-p_c)^2 2 + \ldots + p_c^4 0] = 4p_c(1-p_c^2). \tag{31}$$

The result (30) is, of course, quite general within scheme 1. A direct diagram-by-diagram evaluation of (22) can also be carried out; however, in order to prove $\lambda_t = \lambda_p$ for any cluster, we would like to relate the contributions to (22) and (27), and the difficulty in doing this stems from the fact that the differentiation of P_α in (22) does not bring down a factor obviously related to the r_α of (30). The need for some regrouping of diagrams to obtain the equivalence of contributions to (22) and (27) is thus suggested, and this is the reason other schemes are needed.

Scheme 2 makes the effect of the differentiation of P_α in (22) very simple, and shares an essential aspect (inclusion–exclusion) with scheme 3. We now illustrate its use for the cluster of figure 2. For this cluster, the diagrams of scheme 2 are shown in figure 4. Similar diagrams have been used elsewhere (see, for example, Stinchcombe and Watson 1976). The third diagram is the intersection of the first two, and is drawn in two equivalent forms. The minus sign is that required by the inclusion–exclusion principle in combining probabilities. In scheme 2 only diagrams with $S_\alpha = 1$ have been considered from the outset. The 'probabilities' are $P_1 = P_2 = p^2$ and $P_3 = (-1)p^4$, leading at once, via (19), to (16). Now (22) can be used very simply, since, in scheme 2, $|P_\alpha|$ is the n_αth power of p where n_α is the number of full lines in the diagram, and so

$$P'_\alpha = (n_\alpha/p)P_\alpha. \tag{32}$$

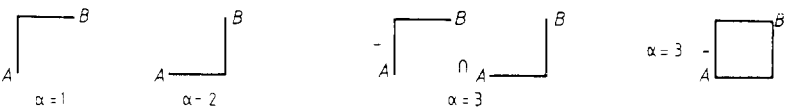

Figure 4. Diagrams of scheme 2 for the simple cluster of figure 2.

Equation (22) therefore takes the form

$$\lambda_p = \frac{1}{p_c} \sum_{\alpha} P_\alpha(p_c) n_\alpha S_\alpha. \tag{33}$$

Like (30) this is again a general result, but it holds in a different scheme; so P_α in (30) and (32) are different, and furthermore n_α and r_α are not simply related. For the diagrams of figure 4, (33) becomes

$$\lambda_p = \frac{1}{p_c} [p_c^2 2 + p_c^2 2 - p_c^4 4] = 4p_c(1-p_c^2). \tag{34}$$

Because of the comments under (33) we would seem to be no nearer finding a general approach to obtaining a cluster-independent equivalence of λ_p and λ_t. However, the regrouping involved in scheme 3 does give the required framework for a general result.

The graphs of scheme 3 are obtained from those of scheme 2 by combining, in the manner of the inclusion–exclusion principle, all intersections of other graphs with a given graph. Thus in our simple illustration we group the scheme 2 graphs (figure 4) as shown in figure 5 to obtain the graphs of scheme 3. The idea is now still to use scheme 2 for the evaluation of λ_p via (33), but to use the new scheme 3 for the evaluation of λ_t, and to show a general relationship between the two schemes, which are obviously more closely related than scheme 1 is to scheme 2. An essential point is that $T'_\alpha(1)$ is still easy to evaluate in scheme 3: the intersections combined with a basic graph to give a graph of scheme 3 correspond to parallel path corrections which do not change $T'_\alpha(1)$ (appendix 1), but of course they do contribute to the probability factor. So, for the graphs of figure 5,

$$P_1 = P_2 = p^2 - p^4 \qquad P_3 = p^4 \tag{35}$$

$$T'_1 = T'_2 = 2 \qquad T'_3 = 0 \tag{36}$$

again giving, through (27), the result $4p_c(1-p_c^2)$ for λ_t.

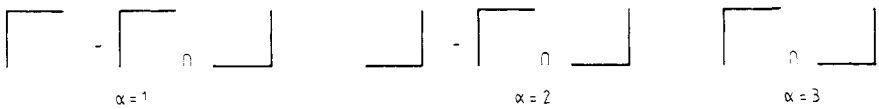

Figure 5. Diagrams of scheme 3 for the simple cluster of figure 2.

The evaluation of λ_p using (33) in scheme 2, and λ_t using (30) in scheme 3, is now given for a more complicated example, employing the twelve-bond cluster of figure 6(a), which can be built up from the series paths $i = 1, 2, 3$ of figure 6(b). The diagrams of scheme 2 are the paths $\{i\}$, and their intersections $\{i \cap j\}$, $\{i \cap j \cap k\}$, as shown in figure 7. The factors in the evaluation of the terms of (33) are shown in table 1

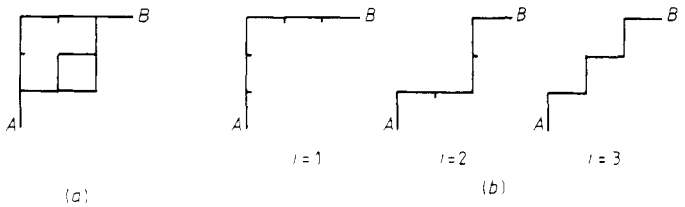

Figure 6. (a) Twelve-bond cluster; (b) the three series paths, $i = 1, 2, 3$, between undecimated spins A and B, which are required to treat the full cluster (a).

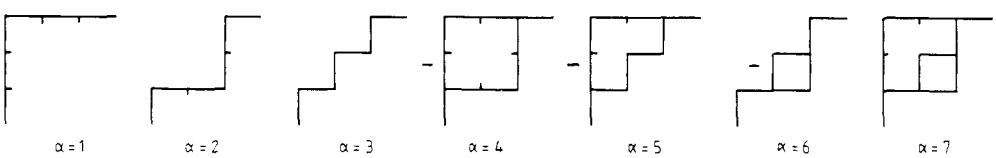

Figure 7. Diagrams of scheme 2 for the cluster of figure 6(a).

($S_\alpha = 1$ for all diagrams drawn). The diagrams of scheme 3 are

$$\left\{i - \sum_{j(\neq i)} i\frown j + \sum_{j>k(\neq i)} i\frown j\frown k\right\} \qquad \left\{i\frown j - \sum_{k(\neq i,j)} i\frown j\frown k\right\} \qquad \{i\frown j\frown k\}$$

as shown in figure 8, and their contributions to (30) are built up in table 2. In this example we thus obtain

$$\lambda_t = \lambda_p = 18p_c^5 - 8p_c^7 - 20p_c^9 + 12p_c^{11}. \tag{37}$$

The next section uses schemes 2 and 3 to establish the equivalence of λ_p and λ_t in general.

Table 1. Evaluation of λ_p using scheme 2 diagrams of figure 7.

α	P_α	n_α
1	p^6	6
2	p^6	6
3	p^6	6
4	$-p^{10}$	10
5	$-p^{10}$	10
6	$-p^8$	8
7	p^{12}	12

$$\frac{1}{p}\sum_\alpha P_\alpha n_\alpha S_\alpha = 18p^5 - 8p^7 - 20p^9 + 12p^{11}$$

Table 2. Evaluation of λ_t using scheme 3 diagrams of figure 8.

α	P_α	r_α
1	$p^6 - 2p^{10} + p^{12}$	6
2	$p^6 - p^8 - p^{10} + p^{12}$	6
3	$p^6 - p^8 - p^{10} + p^{12}$	6
4	$p^{10} - p^{12}$	2
5	$p^{10} - p^{12}$	2
6	$p^8 - p^{12}$	4
7	p^{12}	2

$$\frac{1}{p}\sum_\alpha P_\alpha r_\alpha S_\alpha = 18p^5 - 8p^7 - 20p^9 + 12p^{11}$$

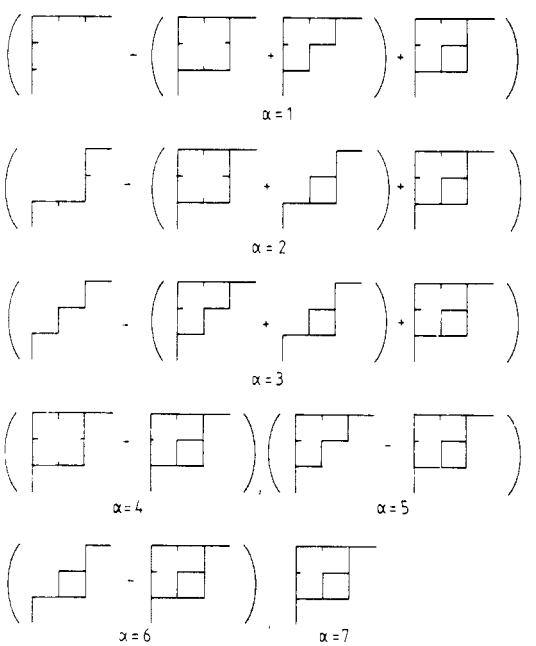

Figure 8. Diagrams of scheme 3 for the cluster of figure 6(*a*).

4. General proof of unit crossover exponent in RSRG

To show that (1) follows quite generally from the RSRG method we have to give a derivation without the restrictions (i) and (ii) at the beginning of § 3.

The procedures developed at the end of § 3 enable us now to remove restriction (i), and to obtain a cluster-independent equivalence between λ_p and λ_t as defined by the first moment approximation (20). We remove the first moment approximation later in this section.

To obtain the equivalence with general clusters we use (33) with scheme 2 for the evaluation of λ_p, and (30) for the evaluation of λ_t in scheme 3, and show the exact equivalence of the two results.

We adopt the notation $\{i\}$ for paths, and $\{i \cap j\}$ for the set of pairwise intersections of those paths, etc, as already introduced in § 3.

The contributions of any cluster are then represented, in both schemes 2 and 3, by a set of paths $\{i\}$ and multiple intersections of those basic paths; only the grouping of the intersections is different in schemes 2 and 3.

In scheme 2 the diagrams are

$$\alpha = \{i\}, -\{i_\cap j\}, \{i_\cap j_\cap k\}, \ldots \tag{38}$$

and the associated probability and bond-number factors are

$$P_\alpha(p_c) = \{P_i = p_c^{n_i}\}, -\{P_{i_\cap j} = p_c^{n_{i_\cap j}}\}, \ldots \tag{39}$$

$$n_\alpha = \{n_i\}, \{n_{i_\cap j}\}, \ldots \tag{40}$$

where we have used $i_\cap j_\cap \ldots$ as a more explicit diagram label than α, and $n_{i_\cap j}$ is the number of bonds in diagram $i \cap j$, etc. Then (33) becomes

$$\lambda_p = \frac{1}{p_c}\left\{\sum_i P_i n_i - \sum_{i>j} P_{i_\cap j} n_{i_\cap j} + \sum_{i>j>k} P_{i_\cap j_\cap k} n_{i_\cap j_\cap k} - \ldots\right\}. \tag{41}$$

In scheme 3, the diagrams and probability factors are

$$\alpha = \left\{i - \sum_{j(\neq i)} i_\cap j + \sum_{j>k(\neq i)} i_\cap j_\cap k - \ldots\right\},$$

$$\left\{i_\cap j - \sum_{k(\neq i,j)} i_\cap j_\cap k + \sum_{k>l(\neq i,j)} i_\cap j_\cap k_\cap l - \ldots\right\},$$

$$\left\{i_\cap j_\cap k - \sum_{l(\neq i,j,k)} i_\cap j_\cap k_\cap l + \ldots\right\}, \ldots \tag{42}$$

$$P_\alpha(p_c) = \left\{p_i - \sum_{j(\neq i)} P_{i_\cap j} + \sum_{j>k(\neq i)} P_{i_\cap j_\cap k}\right\}, \left\{P_{i_\cap j} - \sum_{k(\neq i,j)} P_{i_\cap j_\cap k} + \ldots\right\}, \ldots. \tag{43}$$

We also need the following simple results (appendix 2) for r_α, the numbers of 'disconnecting' single bonds in the basic diagram which, together with its intersections with other diagrams, comprises the full diagram α of scheme 3:

$$r_\alpha = \{n_i\}, \{n_i + n_j - n_{i_\cap j}\}, \{n_i + n_j + n_k - n_{i_\cap j} - n_{i_\cap k} - n_{j_\cap k} + n_{i_\cap j_\cap k}\}, \ldots. \tag{44}$$

Then evaluating (3) in this scheme gives

$$\lambda_t = \frac{1}{p_c}\Big\{\sum_i \Big(P_i - \sum_{j(\neq 1)} P_{i\frown j} + \sum_{j>k(\neq i)} P_{i\frown j\frown k} + \ldots\Big)n_i$$
$$+ \sum_{i>j}\Big(P_{i\frown j} - \sum_{k(\neq i,j)} P_{i\frown j\frown k} + \ldots\Big)(n_i + n_j - n_{i\frown j})$$
$$+ \sum_{i>j>k}(P_{i\frown j\frown k} - \ldots)(n_i + n_j + n_k - n_{i\frown j} - n_{i\frown k} - n_{j\frown k} + n_{i\frown j\frown k}) + \ldots\Big\}. \quad (45)$$

It is now a straightforward exercise to show that (45) reduces to (41), thus proving the equivalence to λ_p, independently of the cluster. Thus, in general

$$\lambda_p = \lambda_t \text{ (first moment)}. \quad (46)$$

It now remains to remove the first moment restriction given as (ii) at the beginning of § 3. The essential points are already included in Young and Stinchcombe (1976), but we give a brief, yet complete, treatment here. The tanh variable t used up to now is strictly the effective value of a bond-random variable, t_i, say (where i now labels a particular bond). This random variable is initially distributed with a binary probability distribution

$$\phi_0(t_i) = (1-p)\delta(t_i) + p\delta(t_i - t). \quad (47)$$

However, after n scalings the distribution takes a non-binary form

$$\phi_n(t_i) = (1-p_n)\delta(t_i) + p_n\theta_n(t_i) \quad (48)$$

where

$$\phi_{n+1}(t_j) = \int \Big(\prod_i \mathrm{d}t_i\Big)\Big(\prod_i \phi_n(t_i)\Big)\delta(t_j - T\{t_i\}). \quad (49)$$

Here the products Π go over all the bonds of the cluster being used in the scaling, and $T\{t_i\}$ is the value of the tanh variable representing the coupling between the undecimated spins (A, B) of the cluster when the bond variables of the cluster take the values $\{t_i\}$. Equation (19) follows exactly from (48) and (49) by picking out the weight p_{n+1} of the terms in (49) which correspond to all the linkages between the undecimated spins: this is done by placing all $t_i = 1$ in the right-hand side of (49) and using (23) (cf below), and identifying the transformation function R from

$$p_{n+1} = R(p_n). \quad (50)$$

Equation (20), is, however, obtained from (49) by making the binary approximation

$$\theta_n(t_i) \sim \delta(t_i - t) \qquad \theta_{n+1}(t_j) \sim \delta(t_j - t') \quad (51)$$

and setting t' so that it gives the correct first moment $\int \mathrm{d}t_i\, \phi_{n+1}(t_j)$ of equation (49) (Stinchcombe and Watson 1976). This is the 'first moment' approximation referred to as restriction (ii).

We now show that this approximation maintains the exact value of λ_t. λ_t is the eigenvalue of the transformation linearised in the low-temperature region. It is possible to show that in this region an initially binary distribution does not depart much from binary form under the transformation (49). To do this we insert into (49)

$$\phi_n(t_i) = (1-p_n)\delta(t_i) + p_n\delta(t_i - t). \quad (52)$$

The two parts of ϕ_n correspond to bond i being absent or present, and when the integrals over $\{dt_i\}$ are carried out in (49) the right-hand side becomes a sum of terms corresponding to all the specific configurations of the cluster obtained by allowing each bond to be present or absent. Any such term would correspond to a configuration listed in scheme 1 and labelled by $\alpha = 1, 2, \ldots$. For each such term the scaled random variable t_j takes the value $T_\alpha\{t_i\}$ where

$$T_\alpha\{t_i\} \equiv T_\alpha(t) \tag{53}$$

and $T_\alpha(t)$ is as used previously. The probability of the term is again $P_\alpha(p)$. The difference from our earlier considerations is that we are now able to see that there are many possible outcomes for t_j, amounting to a non-binary distribution for t_j. However, since the analysis concerns only the low-temperature region, the results (26) and (28) can be used:

$$T_\alpha\{t_i\} = 1 - \varepsilon r_\alpha + O(\varepsilon^2) \tag{54}$$

(again we need only consider configurations α which give a linkage, i.e. for which $S_\alpha = 1$). Since ε is initially small (low temperature), $T_\alpha\{t_i\}$ is close to 1, which means that all the possible (non-zero) values of the scaled t_j are also close to 1. (This is related to the fact that any coupling of spins is enough to make them likely to be parallel at sufficiently low temperatures.) Thus if the initial t_i is given by a binary distribution (52) with t close to 1, the scaled t_j is given by a distribution of the form (48) with $\theta(t_j)$ a function which is only non-zero for t_j very near 1, i.e. again closely approximating a binary distribution of the initial form. This form is therefore approximately preserved; and though the distribution is not strictly binary after scaling, it can be seen from (54) that since ε is small the nth moment of the scaled distribution involves n times the average of r_α over all configurations of the cluster, and so any such measure of the effective value of the scaled exchange gives a result equivalent to (20) in the low-temperature form (27) or, more explicitly, (30). Thus the 'first moment' approximation (ii) is exact for the thermal eigenvalue λ_t of the transformation linearised at the zero-temperature fixed point:

$$\lambda_t\,(\text{first moment}) = \lambda_t. \tag{55}$$

The demonstration, at the beginning of this section, that for any cluster the percolation and 'first moment' thermal eigenvalues are the same (equation (46)), taken together with the result (55) just established thus leads to

$$\lambda_p = \lambda_t \tag{56}$$

$$\phi = 1 \tag{57}$$

for the dilute Ising model as treated by the RSRG method applied to *any* cluster in a restricted parameter space. This is the exact result we set out to show.

5. Discussion

The unit crossover exponent result (1) has been shown quite generally for the dilute Ising model with the RSRG method, except that a restricted parameter space has been used. In a complete calculation on clusters of the full generality discussed here, further

neighbour linkages and correlations will be generated. That is, both the thermal variable t and the concentration variable p become just the first members of extended sets of parameters. The result we have established ignores all other members, and is therefore not a complete position-space proof that $\phi = 1$. Of course, if the one-parameter description is exact in some limit, consideration of that limit would be a possible way of completing the position-space derivation. The work of Reynolds *et al* (1980) has often been taken as evidence that the one-parameter description is asymptotically correct in the limit of large cluster size ($b \to \infty$) suggesting that the extension of our work to that limit completes the derivation. However, the work of Reynolds *et al* is for the case of percolation (the q-state Potts model at $q = 1$) while subsequent work of Tsallis and Levy (1981) indicates that for Potts models at higher q the method will not converge to the exact result as $b \to \infty$. This limit does not therefore seem to provide the extension needed to generalise our discussion. Even if it did, we should encounter other problems: in the limit $b \to \infty$ clusters of arbitrary size would have to be allowed for, in which case r_α in (26), (54), etc, could diverge and the range in which such equations were applicable would presumably shrink to zero. (We stress here firstly that for any finite renormalisation group cluster, the situation considered throughout this paper, r_α is necessarily finite and the thermal percolation crossover considered here can be discussed in terms of just the first-order terms (22) and (27) in the expansions of (19) and (20), i.e. employing in particular (26) and (54) only to first order in ε, which is a crucial aspect of our derivation, and secondly that, though r_α is finite for the renormalisation group clusters, the iteration of the consequent renormalisation group recursion relations generates, as it should, an infinite number of cutting bonds for the real lattice near the percolation threshold.) In summary, our discussion is restricted to a one-parameter space; however, the fact that the ε expansion proof (Stephen and Grest 1977, Wallace and Young 1978) of (1) is not restricted to a simple parameter space suggests that some relatively straightforward extension of our viewpoint should remove the limitation. The most obvious extension ($b \to \infty$) is probably not suitable. Alternatively, we might try extending the work to an unlimited parameter space. We have not been able to do that here, though the form of the arguments given in the first half of § 4 suggests certain possibilities for the inclusion of further neighbour contributions to the thermal and geometrical parameters on an equal footing.

As was pointed out earlier, the dilution considered here is bond dilution. That is sufficient for our purposes, since universality implies that the exponents ν_t and ν_p for the site-diluted case will be the same. However, it should be emphasised that it is much more difficult (impossible ?) to prove the results (56) and (57) in the RSRG scheme with site dilution because, unlike the bond-diluted case, particular clusters do not yield $\phi = 1$ (Yeomans and Stinchcombe 1979) so it is difficult to see a general result emerging when tackled by that route.

Up to now, only the dilute Ising model has been considered here. However, Yeomans and Stinchcombe (1980) also found that a specific cluster calculation for the bond-diluted Potts model gave $\phi = 1$, which suggests that our treatment should generalise to that case. Indeed, the general treatment can easily be extended to all (bond) dilute Potts models, to the dilute anisotropic Heisenberg model, and to other models whose (pure) ground state is separated by a gap from all excited states. This feature leads to the existence of a low-temperature exponential variable, cf (4), and to an immediate generalisation of the results such as (28) where the form of the particular thermal variable enters. In the case of the S-state Potts model, in place of

the t variable,

$$u = \frac{\exp(SK) - 1}{\exp(SK) + (S-1)} \equiv f(K) \qquad K = J/k_B T \tag{58}$$

has to be used (Yeomans and Stinchcombe 1980). The zero-temperature fixed point value of this ($K \to \infty$) is again 1 and results such as (3), (5), (7), (23), (26), (28), (30), (54), etc, follow, as shown in appendix 1, but with the use of

$$\varepsilon = S \exp(-SK) \tag{59}$$

instead of (4). In the case of the dilute anisotropic Heisenberg model, a crossover from isotropic Heisenberg behaviour to Ising-like behaviour occurs as the temperature is lowered, if the anisotropy is sufficiently weak (Stinchcombe 1980a, b), while if the anisotropy is strong the behaviour is always of Ising type. In either case, the limiting thermal–percolation crossover in the neighbourhood of the percolation fixed point is again governed by an Ising-like variable (and all the results of this paper apply) but with an effective exchange depending on the size of the anisotropy. The *isotropic* Heisenberg model does not, however, have unit percolation–thermal crossover exponent since, by virtue of the continuous nature of its excitation spectrum, results such as (28) and (54) do not apply. In this case another exact result can be proved (Stinchcombe 1979, Coniglio 1981a, b) relating its crossover exponent ϕ to the percolative conductivity exponent of the corresponding dilute resistor network.

Appendix 1. Proof of relationship (28)

A proof is given here of the relationship (28) between the contribution $T'_\alpha(1)$ of a cluster configuration α to the thermal eigenvalue and the number r_α of disconnecting single bonds in the cluster configuration as represented in scheme 1.

First consider a diagram of scheme 1 representing a cluster configuration α in which a non-zero exchange from A to B arises via a single path of n bonds in series (possibly with dangling ends, etc) as shown in example (a) of figure 9. Then, by the usual results for decimation of Ising chains (Nelson and Fisher 1975, Young and Stinchcombe 1976)

$$T_\alpha(t) = t^n \tag{A1}$$

$$T'_\alpha(1) = n. \tag{A2}$$

In this example the number r_α of disconnecting bonds is n, since removal of any of the bonds in the series path disconnects A and B; so (A2) establishes (28) for a special case.

Next consider the effect of a parallel constituent in a path of bonds from A to B, as illustrated by example (b) of figure 9, where m, n, r and s label the numbers of bonds in the different parts of the path. Here

$$T_\alpha(t) = t^{m+n} \mathscr{T}_{rs}(t) \tag{A3}$$

where $\mathscr{T}_{rs}$ arises from the parallel part and is given by

$$\mathscr{T}_{rs} = \frac{t^r + t^s}{1 + t^r t^s}. \tag{A4}$$

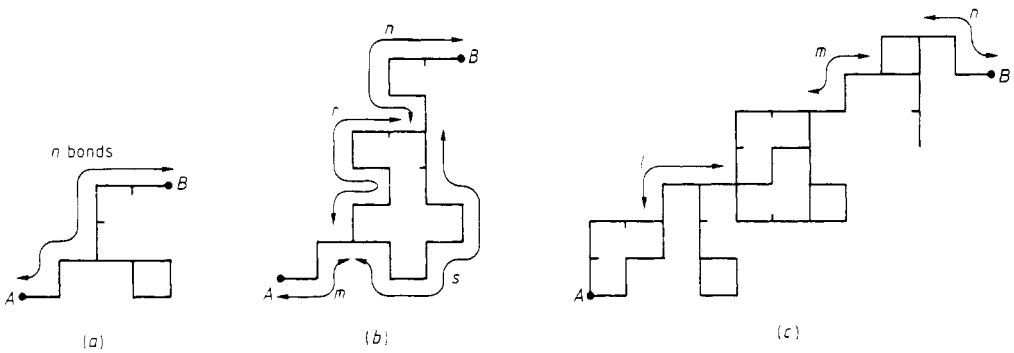

Figure 9. Representative diagrams of scheme 1 to illustrate the proof of (28): (*a*) a diagram in which a single path of bonds in series, with dangling ends, contributes non-zero exchange from A to B, (*b*) a diagram with a parallel constituent in the path of bonds from A to B, (*c*) a more complicated diagram.

It is easy to check that

$$\mathcal{T}'_{rs}(1) = 0 \tag{A5}$$

and so

$$T'_{\alpha}(1) = m + n. \tag{A6}$$

This is again a special case of (28), since the number r_α of disconnecting bonds in figure 9(*b*) is $m+n$.

This result generalises in a straightforward manner to the case where three or more parallel paths of q, r, $s \ldots$ bonds in series occur, when $\mathcal{T}_{rs}$ is replaced by $\tanh(\tanh^{-1} t^q + \tanh^{-1} t^r + \tanh^{-1} t^s + \ldots)$, which again has zero derivative at $t = 1$. If one of the paths added in parallel has itself a parallel insertion, in place of $\tanh^{-1} t^q$ (say) one has instead a term of the form $\tanh^{-1}(t^{q_1+q_2}\mathcal{T}_{s_1 s_2}(t))$ (cf (A3)) and again the parallel parts do not contribute to the derivative $T'_\alpha(1)$.

Thus for a diagram of general form, with various types of parallel connection, dangling bonds, etc, we obtain the required result

$$T'_{\alpha}(1) = r_\alpha \tag{A7}$$

where r_α is the number of disconnecting bonds in the diagram. A typical example is shown in figure 9(*c*), where $r_\alpha = l + m + n$.

The result (A7) can be proved in a similar way for the anisotropic Heisenberg model below its anisotropy crossover temperature, for the Potts model and for other systems with a gap spectrum. For the Potts model, for example, t is replaced by the Potts model variable u defined in (58), and $T_\alpha(t)$ becomes $U_\alpha(u)$ where U_α is the contribution of diagram α to the variable u of the effective bond coupling A and B in the decimated lattice. Then (A1) is replaced by (Yeomans and Stinchcombe 1980)

$$U_\alpha(u) = u^n \tag{A8}$$

and (A3) by

$$U_\alpha(u) = u^{m+n}\mathcal{U}_{rs}(u) \tag{A9}$$

where

$$\mathcal{U}_{rs}(n) = f(f^{-1}(u^r) + f^{-1}(u^s)) \tag{A10}$$

with $f(K)$ as defined in (58). It is easy to show that $\mathcal{U}'_{rs}(1)$ is zero and results analogous to (A6) and (A7) follow in an obvious manner.

From the proof of (A7) (or the analogous proof for the Potts and other 'gap' systems) it can be seen that when (in scheme 3) the inclusion–exclusion combination of paths causes parallel loops to be added to graphs, these have no effect on the contribution to $T'_\alpha(1)$ (or $U'_\alpha(1)$, etc), as stated in the paragraph above (35) and used at various stages in the paper.

Appendix 2. Proof of relationship (44)

A proof is given here of the result (44) for the number r_α of 'disconnecting' bonds in the basic diagram which together with its intersections with other diagrams comprises the full diagram α of scheme 3.

The results (44), and the description of the 'basic' diagram given in the above paragraph, are best illustrated by simple examples. First consider diagram $\alpha = 3$ of figure 8. The first ('sawtooth') member of this diagram (i.e. the path $i = 3$ of figure 6(b)) is here the 'basic' diagram since taken together with its intersections with other paths it leads to all the members of the diagram $\alpha = 3$ of figure 8. In this example the basic diagram is i and the full diagram is

$$\left(i - \sum_{j(\neq i)} i \cap j + \sum_{j>k(\neq i)} i \cap j \cap k\right) \qquad \text{with } i = 3$$

and it is clear that r_α for this basic diagram is just the number n_i of bonds in the sawtooth; this is an illustration of the first parts of equations (42) and (44).

Now consider diagram $\alpha = 4$ of figure 8. The full diagram here is

$$\left(i \cap j - \sum_{k(\neq i,j)} i \cap j \cap k\right)$$

where using the path labelling of figure 6(b) $i = 1$, $j = 2$. The basic diagram is then just $i \cap j$ with $i = 1$, $j = 2$, i.e. diagram 4 of figure 7. This diagram has $r_\alpha = 2$ while according to (44) this basic diagram, being the intersection of two paths, i and j, should have

$$r_\alpha = n_i + n_j - n_{i \cap j} \qquad i = 1,\ j = 2. \tag{A11}$$

That this is so is easily seen by reference to the following diagrammatic form of equation (A11):

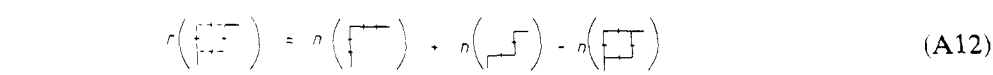

(A12)

where the left-hand side represents the number r_α of disconnecting bonds, shown full in the diagram, and the terms of the right-hand side represent the numbers n_i, n_j, $n_{i \cap j}$ of bonds in the paths i, j and their intersection $i \cap j$. These numbers are, in this case ($i = 1, j = 2$),

$$n_1 + n_2 - n_{1 \cap 2} = 6 + 6 - 10 = 2. \tag{A13}$$

Similarly, for a basic diagram made of an intersection of three paths i, j and k the

result quoted in (44) is

$$r_\alpha = n_i + n_j + n_k - n_{i\frown j} - n_{i\frown k} - n_{j\frown k} + n_{i\frown j\frown k} \tag{A14}$$

which can be illustrated by the example

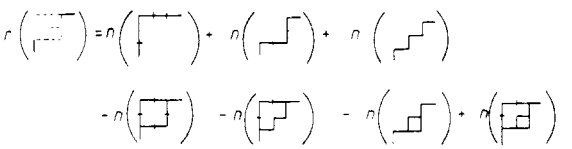

(A15)

$$= 6 + 6 + 6 - 10 - 10 - 8 + 12 = 2. \tag{A16}$$

The general reason for results such as (A11) and (A14) is exhibited by the examples (A12) and (A15): the right-hand sides of (A11) and (A14) are inclusion–exclusion combinations of properties (number of bonds) of a subset (of series paths) and all intersections of members of the subset. By a result of set theory this is the same as the property on the diagrams having only those bonds common to all members of the subset, i.e. the number of series bonds in the basic diagram, which is the number r_α of disconnecting bonds. This is sufficient to establish (44) in general.

References

Coniglio A 1981a *Phys. Rev. Lett.* **46** 250

—— 1981b *Disordered Systems and Localisation* (*Lecture Notes in Physics, vol 149*) ed C Castellani, C di Castro and L Peliti (Berlin: Springer)

Feller W 1968 *An Introduction to Probability Theory and its Applications* vol 1 (New York: Wiley)

Jayaprakash C, Riedel E K and Wortis M 1978 *Phys. Rev.* B **18** 2244

Nelson D R and Fisher M E 1975 *Ann. Phys., NY* **91** 226

Reynolds P J, Stanley H E and Klein W 1980 *Phys. Rev.* B **21** 1223

Stephen M J and Grest G S 1977 *Phys. Rev. Lett.* **38** 567

Stinchcombe R B 1979 *J. Phys. C: Solid State Phys.* **12** 2625

—— 1980a *J. Phys. C: Solid State Phys.* **13** 3713

—— 1980b *J. Phys. C: Solid State Phys.* **13** 3723

—— 1982 *Phase Transitions and Critical Phenomena* vol 7, ed C Domb and J Lebowitz (New York: Academic)

Stinchcombe R B and Watson B P 1976 *J. Phys. C: Solid State Phys.* **9** 3221

Tsallis C and Levy S V F 1981 *Phys. Rev. Lett.* **47** 950

Wallace D J and Young A P 1978 *Phys. Rev.* B **17** 2384

Wilson K G and Kogut J 1974 *Phys. Rep.* **12** 75

Yeomans J M and Stinchcombe R B 1978 *J. Phys. C: Solid State Phys.* **11** L525

—— 1979 *J. Phys. C: Solid State Phys.* **12** 347

—— 1980 *J. Phys. C: Solid State Phys.* **13** L239

Young A P and Stinchcombe R B 1976 *J. Phys. C: Solid State Phys.* **9** 4419